Iranian Journal of Chemical Engineering

Methane Oxy-Steam Reforming Over a Highly Efficient Ni/Al$_2$O$_3$ Nanocatalyst Prepared by Microwave-Assisted Impregnation Method

S. M. S. Hosseini [1], H. Hashemipour [1], A. R. Talebizadeh [2*]

[1] Department of Chemical Engineering, Faculty of Engineering, Shahid Bahonar University of Kerman, Kerman, Iran

[2] Department of Chemical Engineering, Faculty of Engineering, Vali-e-Asr University of Rafsanjan, Rafsanjan, Iran

ARTICLE INFO

ABSTRACT

An alumina-supported nickel catalyst was prepared by impregnation of Ni^{2+} solution onto mesoporous alumina undermicrowave irradiation (denoted as M-Ni/Al$_2$O$_3$). For comparison, a catalyst with the same nickel content was prepared by conventional impregnation method (denoted as UM-Ni/Al$_2$O$_3$). Both M-Ni/Al$_2$O$_3$ and UM-Ni/Al$_2$O$_3$ catalysts were applied to the syngas (H$_2$ + CO) production by methane oxy-steam reforming in order to investigate the effect of preparation method on the catalytic performance.The reaction experiments were performed in a fixed-bed continuous flow reactor under atmospheric pressure. M-Ni/Al$_2$O$_3$ catalyst exhibited higher methane conversion (X$_{CH4}$: 0.94) than UM-Ni/Al$_2$O$_3$ (X$_{CH4}$: 0.58) in the oxy-steam reforming reaction. In addition, the value of syngas yield in M-Ni/Al$_2$O$_3$ (3.21 mole per mole of methane) was almost twice that of one for UM-Ni/Al$_2$O$_3$ catalyst (1.59 moles per mole of methane). Various operating conditions, such as the influences of the O$_2$/CH$_4$ and H$_2$O/CH$_4$ feed ratios, temperature and GHSV on the methane conversion and yield of products were investigated. According to the structural characterization (FTIR, XRD, N$_2$ adsorption/desorption, H$_2$-TPR and TEM), the excellent catalytic performance of M-Ni/Al$_2$O$_3$ catalyst was reasonably attributed to the nano-sized and uniform distributed nickel species (<6 nm) which interacted with the alumina support strongly.

1. Introduction

In recent years, new and different technologies have been developed to produce syngas (a powerful reactive gas) from natural gas. This gas mixture (H$_2$ and CO) is used in different chemical industries to produce ammonia, methanol, and other petrochemicals as well as hydrogen in fuel cells. In addition, syngas is playing a growing role in the energy sector, because it can be converted into a number of important energy carriers and fuels [1-3].

Methane steam reforming (MSR) process is a conventional and traditional technology for

---

producing hydrogen and syngason on industrial scale. MSR is a very energy-intensive process because of the highly endothermic nature of the reactions, hence requiring a significant heat supply facility (such as heat-exchanger) [4]. Consequently, a reformer unit becomes very massive and heavy, and it is not suitable for a mobile fuel cells. On the other hand, catalytic partial oxidation of methane (CPOM) is slightly exothermic and happens 10-100 times faster than the steam reforming, allowing the use of small reactors. Thus, this process is an appropriate approach to producing syngas with low investment and simple equipment [5, 6]. However, CPOM can show several problems, including risk of explosion, hot spot, and low H_2/CO ratio, restricting its applications.

The combination of the CPOM and MSR reactions is called autothermal reforming or, alternatively, methane oxy-steam reforming (MOSR) which is an advanced process in syngas production according to economic and technical reasons. It has low-energy consumption due to the reverse contribution of the endothermic steam reforming and exothermic partial oxidation or total combustion (related reactions are shown in equations: 1-4).

$$CH_4 + H_2O \leftrightarrow CO + 3H_2$$
$$\Delta H = +206 kJ/mol \quad H_2O + CO \leftrightarrow H_2 + \tag{1}$$

$$CO + H_2O \leftrightarrow CO_2 + H_2$$
$$\Delta H = -41.2 kJ/mol \tag{2}$$

$$CH_4 + 2O_2 \leftrightarrow CO_2 + 2H_2O$$
$$\Delta H = -802 kJ/mol \tag{3}$$

$$CH_4 + 0.5O \leftrightarrow CO + 2H_2 \tag{4}$$
$$\Delta H = -36 kJ/mol$$
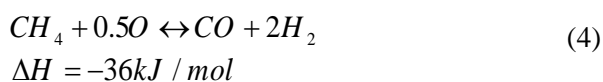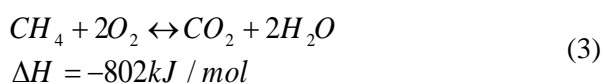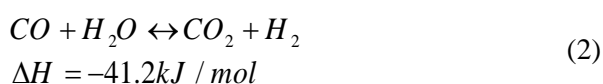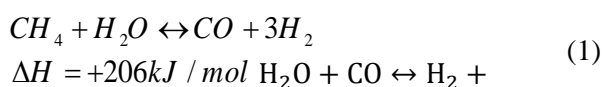
This condition causes a reducation in the hot spots formation and prevention of catalyst deactivation by sintering or carbon deposition. Additionally, MOSR produces more hydrogen related to CPOM due to the water gas shift reaction. Furthermore, a reformer unit based on the MOSR reaction could provide hydrogen with low cost and compact equipment, rapid start-up, more likely for fuel cell electric vehicles [8-14].

In methane oxy-steam reforming, like all other hydrogen and syngas production methods, catalyst has the main role in the efficiency process. Supported metal catalysts, especially alumina supported Ni catalysts, have predominantly received significant attention because of their operational applications in these processes [15-17]. The practical challenge of supported metal catalyst preparation is how to prepare the smallest, most stable metal particles by the simplest and cheapest method. Although the impregnation method gives a catalyst with low quality due to the sintering and coking, this method is the simplest and most prevalent among the others for producing supported metal catalysts. It should be mentioned that this method still has high acceptability in the industry, and it can be modified with special techniques. Recently, chemical strategies have been investigated for modifying the impregnation method to inhibit the formation of larger metal particles and improve metal accessibility to reactants. These strategies involve changes of metal salt precursor, change of impregnation solvent, and addition of some organic additive to the impregnation solution [18-22]. However, these methods have been limited to industrial applications because of the complexity, high cost, and hazardous environmental consequences due to the toxic compounds or toxic gas release.

Microwave-assisted methods have been widely used for the synthesis of organic, inorganic, and hybrid materials. The fast and uniform heating of the reaction medium by microwave radiation enhanced reaction kinetics and also led to the formation of products with uniform size/shape [23]. Various nanostructures of metals, semiconductors, and oxides have been synthesized using microwave-assisted methods [24].

In an applied research, microwave-assisted deposition of noble metal (Pt, Au) nanoparticles on different supports has been reported, predominantly employing solutions of metal salts as precursors. In this method, microwave irradiation was exclusively used for the direct reduction of noble metal precursor and homogeneous nucleation of the metal on the support, which causes short reaction time and production of a set of active sites with narrow-sized distribution and high catalytic activity [25]. Microwave drying provides another technique to reach a catalyst with homogeneous distributions of the metal active sites. It has the potential to speed up drying drastically due to the volumetric heating of the material, removing the need for heat transport from the outer edge of the particle toward the center. Liu et al. studied microwave drying on the pellets impregnated with different concentrations of nickel nitrate solutions [26].

The aim of this work is to modify the wet impregnation method by microwave irradiation for preparing a Ni/Al$_2$O$_3$ nanocatalyst with high catalytic performance and produce syngas with high yield through methane oxy-steam reforming.

2. Experimental
2.1. Catalyst preparation

An alumina-supported nickel catalyst (Ni/Al$_2$O$_3$) was prepared by microwave-assisted wet impregnation method. The support was prepared using Puralox 200 Sba (γ-Al$_2$O$_3$, 200 m$_2$/g and 1.8 mm sphere) from Sasol previously calcined at 600 ^{o}C for 5 h. γ-Alumina was impregnated using an aqueous solution of Ni (NO$_3$)$_2$·6H$_2$O (Merck Company). The concentration of the solution was such that the final catalyst would have a Ni content of 10 wt %. The alumina support was introduced into the solution in a ratio of 1 g of Al$_2$O$_3$ to 10 ml of solution. The mixture was stirred in a microwave oven operating at 2.45 GHz, 200 W at ambient pressure. This step continued until the whole of the solvent evaporated, and the product was completely dried. Then, the dried sample was calcined for 4 h at 500 ^{o}C, and then crushed and sieved to mesh size of 120-50 (125-300 micron). An unmodified catalyst was prepared by a unmodified wet impregnation method according to the procedure described in the literature [27]: a quantity of Ni (NO$_3$)$_2$.6H$_2$O was dissolved completely in 10 ml distilled water, and then 1 g of Al$_2$O$_3$ was introduced into the reaction vessel. The resulting suspension was stirred for 72 h to complete the metal ion deposition on the support. Then, the excess solvent was evaporated under stirring at 100 ^{o}C to obtain a wet solid. This product dried in the oven for 24 h at 100°C and, finally, calcined for 4 h at 500 ^{o}C. For the sake of convenience, the modified and unmodified catalysts are denoted by M-Ni/Al$_2$O$_3$ and UM-Ni/Al$_2$O$_3$, respectively.

2.2. Catalyst characterization
X-ray diffraction (XRD) was used to investigate the crystalline phases of Ni species in the catalysts. The XRD patterns were collected by a D$_8$-Advance Bruker

diffractometer with Cu Kα radiation (λ=1.5406 Å) in a step scanning mode over 2θ angle between 10° and 80° at a scan speed of 1.5°/min. The functional groups of the catalysts were gained by Fourier-transformed infrared spectroscopy (FTIR) using a Matson 1000 spectrometer. The specific surface areas and pore size distributions of the calcined catalyst were measured by the analysis of nitrogen isotherms collected at 77 K using a BEL Sorp adsorption-desorption apparatus. The reduction behavior of the catalyst was characterized using temperature-programmed H_2 reduction (H_2-TPR). The TPR test was carried out by the following procedure: 50 mg of each sample was loaded into a U-shaped quartz reactor and heated up to 1000 ^{o}C in a flow of 7 % H_2/Ar gas mixture (20 ml/min) and at a heating rate of 10 ^{o}C/ min. The consumption of H_2 was monitored with a thermal conductivity detector (TCD). The catalyst morphology was obtained by transmission electron microscopy (TEM) using a Philips CM20 instrument. Before TEM analysis, the catalysts ultrasonically dispersed in ethanol and the obtained suspension deposited on a carbon-coated copper grid.

2.3. Catalyst testing

Fig. 1 shows schematic diagram of the experimental setup of the reaction. The reaction was carried out in a quartz fixed-bed micro reactor with a 7.0 mm inner diameter and 43 cm length at atmospheric pressure. The reaction temperature was controlled by an electrical tube furnace and a digital temperature controller. The flow rates of the gases and water were adjusted by mass flow controllers and syringe pump, respectively. In each experiment, 60 mg of the catalyst was loaded into the reactor. After loading, the catalyst was reduced according to the following procedure: the catalyst bed was heated to 600 ^{o}C in an Ar atmosphere with a heating rate of 10 ^{o}C/ min. Then, a H_2 stream diluted with Ar (30 %) was passed over the catalyst for 1 h. After that, the bed temperature increased to reaction temperature at a heating rate of 10 ^{o}C/ min. Then, a gas feed, consisting of CH_4, O_2, H_2O, and Ar (high pure 99.999 %), was entered into the reactor. The water vapor in the product stream was completely condensed and separated by cold trapping. The required cooling was obtained by a refrigerated bath circulator. The reaction products were analyzed by an online gas chromatograph (GC-2550 TG) equipped with a TCD using Ar as the carrier gas. The mass balance of carbon was measured during reaction whose parameter was always within a ±5 % error range. The catalyst performance was analyzed in terms of methane conversion (X_{CH4}), moles of produced hydrogen (nH_2), moles of produced carbon monoxide (nCO), and moles of produced carbon dioxide (nCO_2) per mole of methane in the feed, respectively, which are calculated as follows:

$$X_{CH_4} = \frac{y_{CO} + y_{CO_2}}{y_{CO} + y_{CO_2} + y_{CH_4}}$$

$$n_{H_2} = \frac{y_{H_2}}{y_{CO} + y_{CO2} + y_{CH_4}}$$

$$n_{CO} = \frac{y_{CO}}{y_{CO} + y_{CO_2} + y_{CH_4}}$$

$$n_{syngas} = \frac{y_{CO} + y_{H_2}}{y_{CO} + y_{CO_2} + y_{CH_4}}$$

where y_{CO}, y_{CO_2}, y_{H_2}, and y_{CH_4} are components of volume fractions in the outlet gas flow.
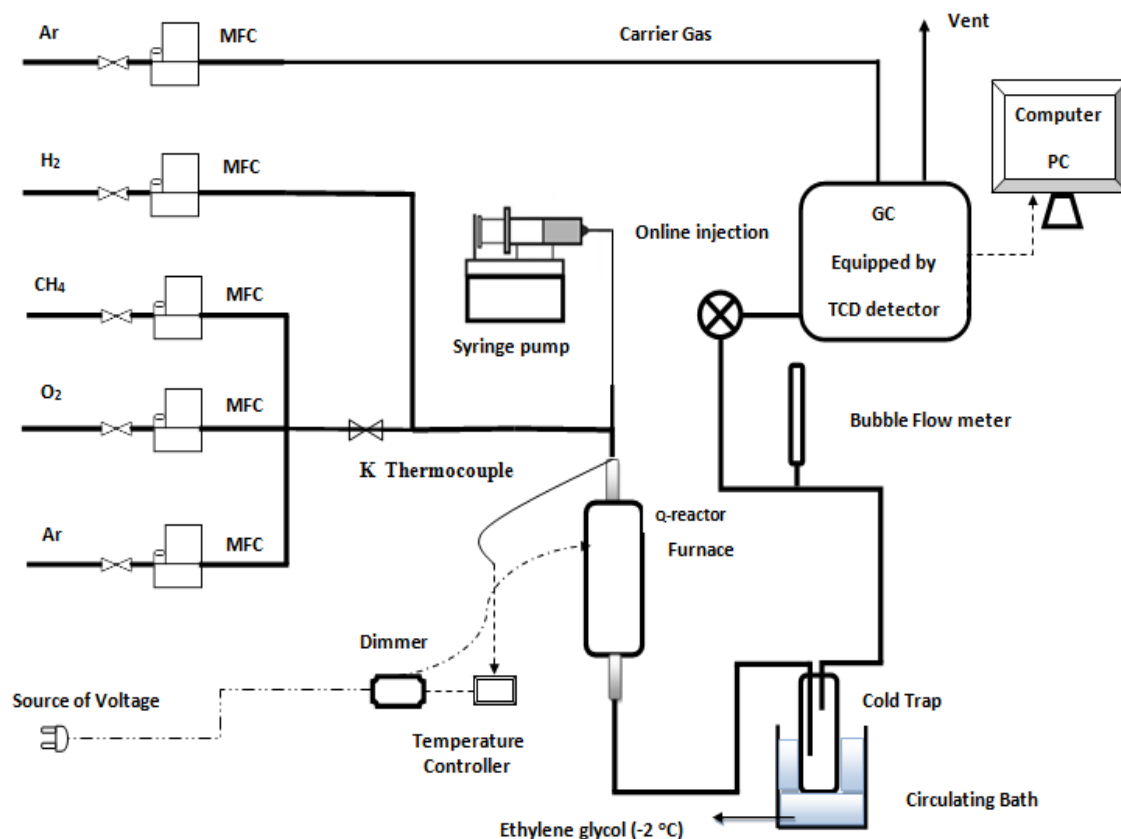
Figure 1. Schematic diagram for the reaction set up.

3. Results and discussion

3.1. Catalyst performance

The catalytic performances of M-Ni/Al$_2$O$_3$ and UM-Ni/Al$_2$O$_3$ in methane steam reforming (MSR), catalytic partial oxidation of methane (CPOM) and methane oxy-steam reforming (MOSR) are shown in Table 1.

Table 1

Catalytic performance of UM-Ni/Al$_2$O$_3$ and M-Ni/Al$_2$O$_3$, T: 750 °C, GHSV= 20 ×10^4 (ml/g.h) and molar ratio in feed: MSR: CH$_4$/ H$_2$O = 1/1, MOSR: CH$_4$/ O$_2$/ H$_2$O = 1/ 0.5/ 1, POM: CH$_4$/O$_2$ =1/ 0.5.

Sample	Reaction	X_{CH_4}	n_{H_2}	n_{CO}	n_{syngas}
	MSR	0.37	1.41	0.22	1.63
UM-Ni/Al$_2$O$_3$	CPOM	0.52	0.71	0.455	1.165
	MOSR	0.58	1.29	0.30	1.59
	MSR	0.51	1.42	0.35	1.77
M-Ni/Al$_2$O$_3$	CPOM	0.96	1.83	0.91	2.74
	MOSR	0.99	2.44	0.77	3.21

In general, we find that M-Ni/Al$_2$O$_3$ is a more effective catalyst than UM-Ni/Al$_2$O$_3$ for all the three reactions. Although the highest amount of the methane conversion and hydrogen production is related to the oxidative steam reforming of methane, it

seems that it enhances the methane oxy-steam reforming over the modified catalyst mainly due to the partial oxidation.

In the case of unmodified catalyst, the methane conversion in partial oxidation was greater than steam reforming, but the amount of hydrogen production was lower. The reason for this behavior is that all of the reacted methane in partial oxidation was not converted to syngas, and a portion of them was converted into CO_2 and H_2O due to total combustion. Based on this behavior, UM-Ni/Al_2O_3 was a moderate catalyst for the methane oxy-steam reforming.

In the case of modified catalyst, the methane conversion and the amount of hydrogen producing in partial oxidation was higher than steam reforming. Also, the syngas ratio obtained in the partial oxidation reaction was the value of 2, indicating that all of the reacted methane was converted into the hydrogen and carbon monoxide according to the reaction stoichiometry (eq. 4). Therefore, $M-Ni/Al_2O_3$ was an efficient catalyst for the methane oxy-steam reforming due to high conversion, resulting from the partial oxidation reaction.

In order to investigate the catalyst stability, two catalyst samples were exposed in a flow of feed with 9/1/5 ratio of $H_2O/O_2/CH_4$ at 850 ^{o}C for 36 h.

As it can be seen from Fig. 2, the modified catalyst has a high catalytic stability for methane oxy-steam reforming, because the methane conversion (X CH_4), syngas yield (n S.G), and syngas ratio (H_2/CO) remained constant during 36 h reaction time on stream. However, UM-Ni/Al_2O_3 catalyst shows lower activity and stability.

Generally, as the time passes, catalysts of reforming process may be deactivated; consequently, process performance index will

drop. Deposition of coke on catalyst surface is the main reason of catalysts deactivation.
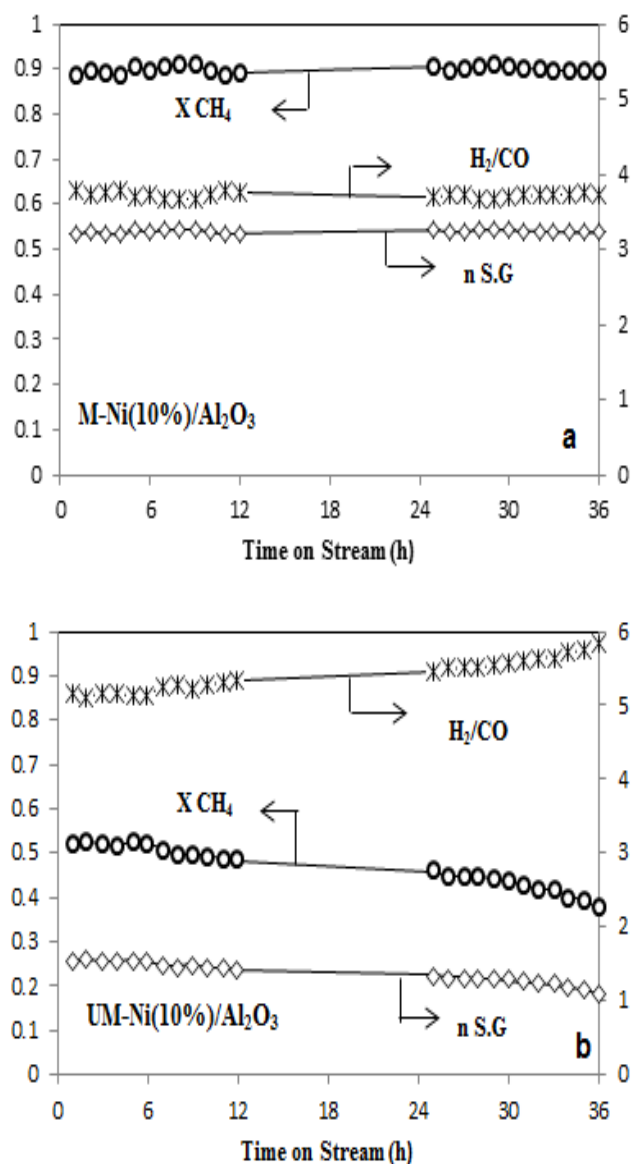
Figure 2. Stability of a) M-Ni/Al_2O_3 and b) UM-Ni/Al_2O_3 in methane oxy-steam reforming CH_4: H_2O: O_2: 5:9:1, T: 850 ^{o}C, GHSV: 20 $\times 10^4$ (ml/g.h).

The constant rate of surface reaction over a catalyst is defined as follows:

$$k = k_0 \psi e^{-\frac{E}{RT}} \tag{5}$$

where ψ represents the catalyst activity.

Assuming that every each active site on the catalyst is covered by carbon, the term for

catalyst activity (ψ) at any time is defined as follows:

$$\psi = \frac{\alpha_0 - \gamma}{\alpha_0} \qquad (6)$$

where α_0 is the number of total active site, and γ is the number of active site covered by carbon.

Thermogravimetric analysis of the used M-Ni/Al₂O₃ catalyst after 36 h of methane oxy-steam reforming did not show any weight loss related to coke oxidation. It seems that the carbon deposition on the active sites is negligible ($\gamma = 0$ so $\psi = 1$), and the rate of catalyst deactivation is zero. Accordingly, M-Ni/Al₂O₃ showed a stable catalytic performance during 36 h reaction time on stream.

In this section, the effect of operating conditions on methane oxy-steam reforming over M-Ni/Al₂O₃ catalyst is investigated. Fig. 3 shows the experimental results of the catalyst performance as a function of O_2/CH_4 and H_2O/CH_4 feed ratios.

Methane conversion increased with the increase of O_2/CH_4 ratio. This effect is related to the improvement of the partial oxidation reaction. O_2/CH_4 ratio of zero (steam reforming) methane conversion is 0.5, while this parameter has almost increased to unity in O_2/CH_4 ratio of 0.5.

Water addition has the overall effect of increasing yield of H_2, decreasing yield of CO and increasing yield of CO_2.

According to Souza research [29], the best ratio for feed composition to avoid coke deposition in methane oxy-steam reforming is 5:1:9 for $CH_4/O_2/H_2O$. Considering this ratio, the study of the effect of temperature and space velocity (GHSV) on the reaction was carried out.
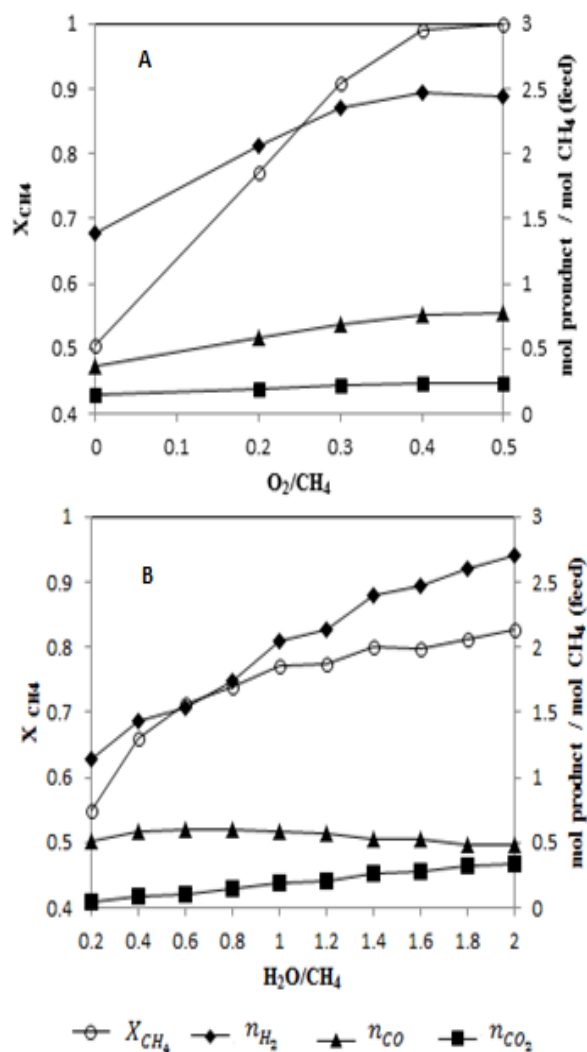
Figure 3. (A) effect of O_2/CH_4 ratio and (B) H_2O/CH_4 ratio on the catalytic performance of M-Ni/Al₂O₃ in methane oxy-steam reforming, T: 750 °C, GHSV: 20×10^4 (ml/g.h), CH_4/H_2O: 1/1.

As in Fig. 4, methane conversion increased with increase of the reaction temperature and reasonably the yield of H_2 and CO increased. In addition, with the increase of temperature, the yield of CO_2 decreased. These results indicate that, in the higher temperature, the CPOM reaction is more effective than MSR and WGS reaction. Increasing the temperatures leads to the decrease in H_2/CO due to the fact that the WGS reaction is thermodynamically unfavorable at higher temperatures.
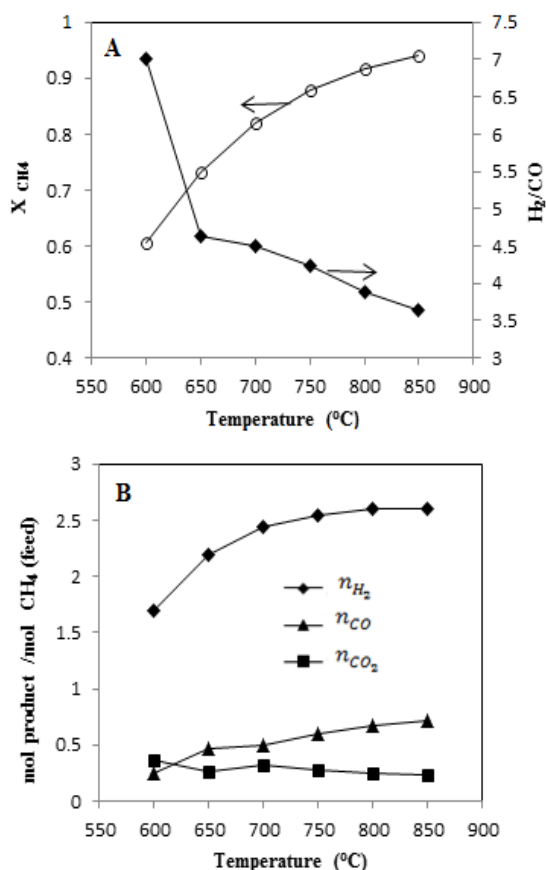
Figure 4. Effect of temperature on the catalytic performance of M-Ni/Al$_2$O$_3$ in oxy-steam reforming, CH$_4$: H$_2$O: O$_2$: 5:9:1, GHSV: 10×10^4 (ml/g.h), A) X$_{CH_4}$, H$_2$/CO ratio, B) n$_{H_2}$, n$_{CO}$, n$_{CO_2}$.

The results in Fig. 5 show that increasing the space velocity causes a decrease in methane conversion and in the yield of the main products due to decrease in the residence time. In addition, with increasing the space velocity, the ratio of H$_2$/CO slightly increases, which can be due to the occurrence of the water-gas shift reaction in the higher space velocity.

3.2. Modified catalyst characterization

Characterization analyses of the modified Ni/Al$_2$O$_3$ catalyst in terms of FTIR, XRD, pore size distribution and H$_2$-TPD are presented in Figure 6(a-d). A sharp band around 1380 cm^{-1} is seen in the FTIR spectra of the dried catalyst (Fig. 6-a), indicat the

presence of NO$_3^-$ after the precursor salt impregnation [30]. This band is completely removed from the calcined sample, indicating that, after calcination treatment, the loaded nickel nitrate almost decomposed to nickel oxide linked to the support without any counterions' interaction. A broad band at around 3443 cm^{-1} arises from the stretching vibration of hydrogen bonded hydroxyl groups, and the absorption band at 1640 cm^{-1} is due to the bending vibration of adsorbed water. These vibrations are seen with less intensity in calcined sample due to the elimination of free or crystalline water molecules. In the calcined sample, the absorption bands appearing at ~637, ~748 cm^{-1} and ~810 represent Al-O and Ni-O vibrations in octahedral and tetrahedral structures [31, 32].
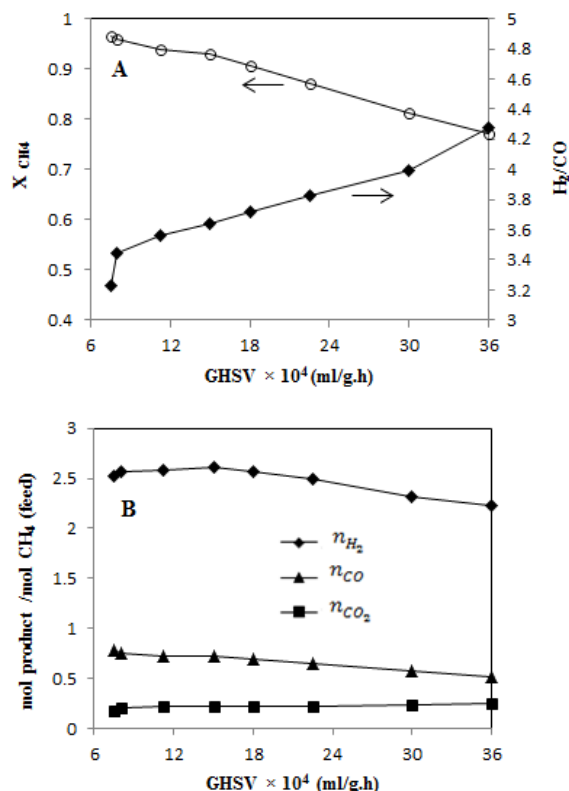
Figure 5. Effect of GHSV on the catalytic performance of M-Ni/Al$_2$O$_3$ in the methane oxy-steam reforming, A) X$_{CH_4}$, H$_2$/CO ratio and B) n$_{H_2}$, n$_{CO}$, n$_{CO_2}$. , CH$_4$: H$_2$O: O$_2$: 5:9:1, T: 850 °C.

By comparing the XRD patterns of the alumina support and calcined catalyst (Figure 6-b), the peaks attributed to alumina phase, obviously, are detectable in the catalyst and the peaks related to NiO phase are broad and hardly seen (shown with arrows). The (200) reflection of NiOis seen better among diffraction peaks related to Al_2O_3 and it can be reasonably used to evaluate the average size of NiO nanoparticles detected by XRD according to Scherrer equation (Table 2). This parameter obtained almost 4.6 nm, which indicates that the size of distributed NiO species on alumina is very small.
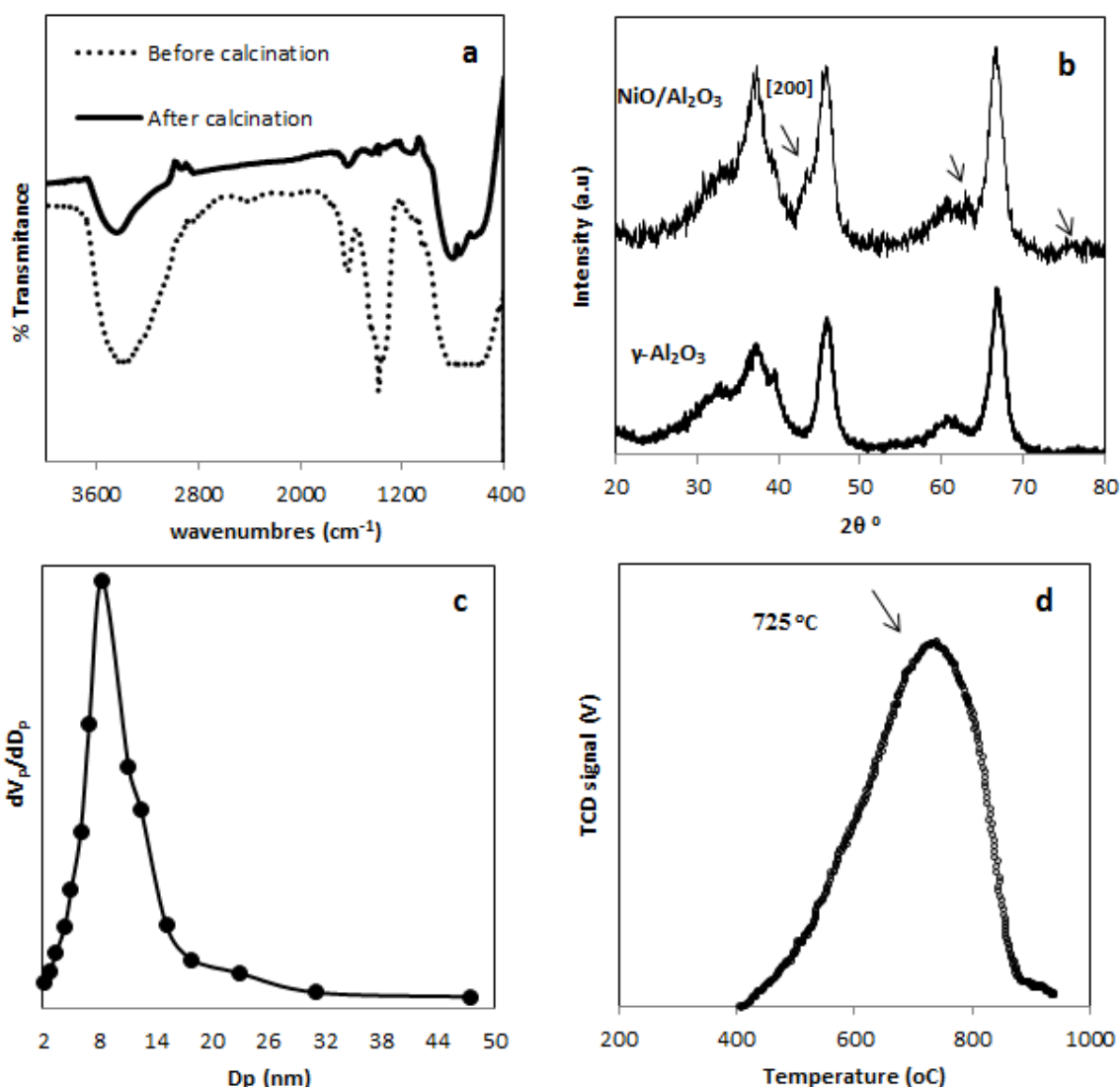
Figure 6. Characterization analyses of the modified Ni/Al₂O₃ catalyst: a) FTIR spectra before and after calcination, b) XRD patterns of alumina and catalyst (NiO phases are shown with arrows), c) pore size distribution, and d) H₂-TPR.

Figure 6-c shows pore size distribution of the catalyst obtained from N₂-adsorption /desorption isotherms based on BJH method. As can be seen, this distribution is quite narrow with maximum pore diameters of 8.3 for the catalyst. This result could be due to the good dispersion of nickel species on all alumina surfaces. BET surface area, pore volume and mean pore diameter of γ-Al₂O₃ and Ni/Al₂O₃ are shown in Table 2. The

decrease in the mean pore diameter after the nickel loading displayed that most of the pores are still accessible and little pore blockage occurs.

Table 2
Results of BET surface area, pore volume and pore diameter of γ-Al_2O_3 and the modified catalyst.

sample	S_{BET} (m^2/g)	Pore volume (cm^3/g)	Pore diameter (nm)	d_{XRD} (nm)	Reduced NiO (%)
γ-Al_2O_3	200	0.73	10	-	-
NiO/Al_2O_3	186	0.61	8.3	4.6	85

TPR analysis is used mainly in catalysis research to evaluate the interaction of active metal site with the oxide support [33]. The TPR profile of catalyst (Figure 6-d) exhibits one peak at 725 ^{o}C and no peak is observed below this temperature. According to the literature reviews [34], the reduction peaks observed below T: 500 ^{o}C can be ascribed to the reduction of larger NiO species that interacted with the support weakly or bulk NiO particles, whereas the peaks observed above T: 500 ^{o}C can be attributed to the reduction of smaller NiO species that interacted with the support strongly. In addition, The TPR profile of the catalyst is sharp and well defined which could be due to the presence of a narrow population of Ni species. All these results indicate that the modified catalyst is composed of small homogeneous Ni species that strongly interact with alumina surfaces. Almost major amount of the NiO species in the catalyst (85 %) was reduced, indicating suitable reducibility.

XRD analyses reasonably indicated that the NiO species in M-Ni/SiO_2 are very small, whose result is obviously proved by TEM image. Figure 7 gives the TEM images of the modified catalyst (M-Ni/Al_2O_3). It is clearly seen that NiO nanoparticles (less than 6 nm) are uniformly dispersed in the catalyst.
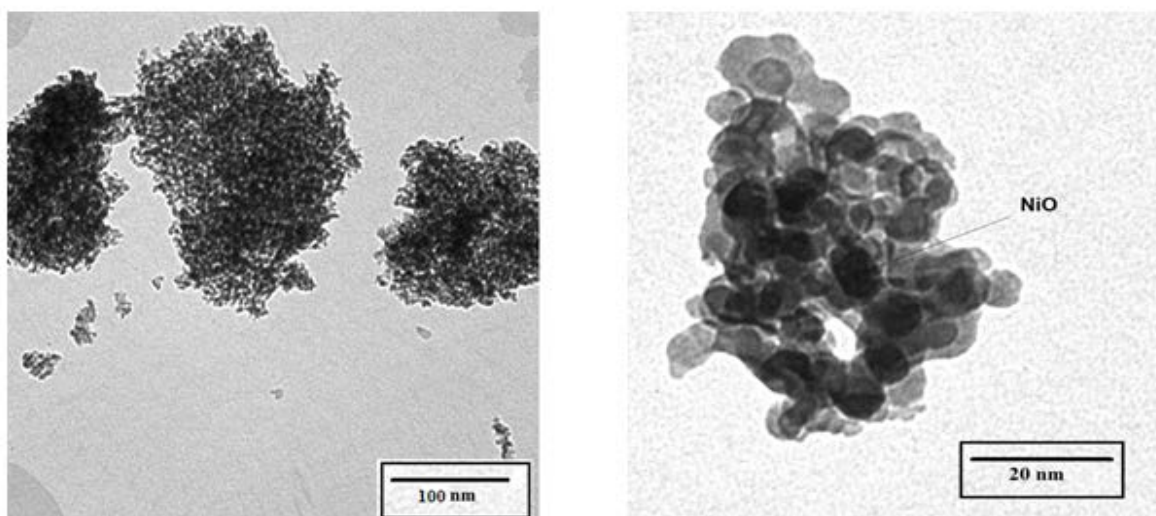

Figure 7. TEM images of M-Ni/Al_2O_3, A) low magnification, B) high magnification.

According to the mentioned results, the catalyst structure was modified using the microwave irradiation. In the first step of the impregnation method, the distribution of the nickel ions inside the wet porosity of the particle was expressed by two phenomena: diffusion of the nickel ions into the alumina pores and interaction of the nickel ions with the alumina specific sites [35]. These phenomena have a lasting influence on the properties of the final catalyst, especially on the nature of the phases resulting from subsequent calcinations treatment [36]. It seems that the microwave irradiation could improve and accelerate the kinetics of these phenomena. In addition, the drying method applied to impregnated support has a significant influence on the size and nickel distribution, where the use of microwave heating (volume heating) for drying the catalyst could prevent agglomeration of nickel species and lead to a better homogeneous dispersion of the active site in comparison with the conventional heating.

4. Conclusions

In this work, a modified supported nickel catalyst was prepared by a wet impregnation method using Ni $(NO_3)_2.6H_2O$ as a nickel precursor, γ-Al_2O_3 as a support, and microwave irradiation as a promotional agent. The catalyst performance was evaluated for the methane oxy-steam reforming, and results showed excellent activity and stability related to the unmodified catalyst. The results demonstrated that the modified catalyst enhanced partial oxidation significantly and steam reforming slightly, in which the combination of these two behaviors led to the increase of methane conversion and suitable H_2/CO ratio in the methane oxy-steam reforming reaction.

The excellent catalytic performance of the modified catalyst was reasonably attributed to the small and uniform distributed Ni species on the support. These special characteristics were derived from microwave irradiation during catalyst synthesis. The use of microwave in the impregnation method led to a strong interaction between Ni ions and alumina and a decline in reaction time, while, in unmodified procedure, Ni deposition was slow and required several hours or days. In addition, the use of microwave heating in the drying step could be another reason for the excellent properties of the modified catalyst.

References

[1] Jens Rostrup-Nielsen, J. and Christiansen, L. J., Concepts in Syngas Manufacture, Imperial College Press, (2011).

[2] Makvandi, S. and Alavi, S. M., "CO$_x$ free hydrogen production by catalytic decomposition of methane over porous Ni/Al₂O₃ catalysts", *Iranian Journal of Chemical Engineering*, **8**, 24 (2011).

[3] Shrif, O. Z., Orhan, M. F. and Dicks, A. L., "An overview of fuel cell technology: Fundamentals and applications", *Renew. Sustainable Energy*, **32**, 810 (2014).

[4] Pino, L., Recupero, V., Beninati, S., Shukla, A. K., Hegde, M. S. and Bera, P., "Catalytic partial-oxidation of methane on a ceria-supported platinum catalyst for application in fuel cell electric vehicles", *Appl. Catal. A: General*, **225**, 63 (2002).

[5] Tanaka, H., Kaino, R., Nakagawa, Y. and Tomishige, K., "Comparative study of Rh/MgO modified with Fe, Co or Ni for the catalytic partial oxidation of methane at short contact time. Part II: Catalytic performance and bed temperature profile", *Appl. Catal. A: General*, **378**,

187 (2010).

[6] Akhlaghian, F., Towfighi, J. and Mohajeri, A., "Partial oxidation of methane on Rh/TiO$_2$ catalysts: Effects of the titania precursor and the presence of tungsten oxide", *Scientia Iranica C*, **19** (6), 1608 (2012).

[7] Santos, D., Madeira, L. and Passos, F., "The effect of the addition of Y$_2$O$_3$ to Ni/α-Al$_2$O$_3$ catalysts on the autothermal reforming of methane", *Catal. Today*, **149**, 401 (2010).

[8] Souza, A., Maciel, L., Lima Filho, N. and Abreu, C.,"Catalytic activity evaluation for hydrogen production via autothermal reforming of methane", *Catal. Today*, **149**, 413 (2010).

[9] Mosayebi, Z., Rezaei, M., Biabani, A. and Hadian, N.,"Autothermal reforming of methane over nickel catalysts supported on nanocrystalline MgAl$_2$O$_4$ with high surface area", *Int. J. Hydrogen Energy*, **37**, 1236 (2012).

[10] Amjad, S., Vita, A., Galetti, C., Pino, L. and Specchia, S., "Comparative study on steam and oxidative steam reforming of methane with noble metal catalysts", *Ind. Eng. Chem. Res.*, **52**, 15428 (2013).

[11] Ismagilov, I. Z., Matus, E. V., Kuznetsov, V. V., Mota, N., Navarro, R. M., Yashnik, S. A., Prosvirin, I. P., Kerzhentsev, M. A., Ismagilov, Z. R. and Fierro, J. L. G.,"Hydrogen production by autothermal reforming of methane: Effect of promoters (Pt, Pd, Re, Mo, Sn) on the performance of Ni/La$_2$O$_3$ catalysts", *Appl. Catal. A: General*, **481**, 104 (2014).

[12] Vita, A., Cristiano, G., Italiano, C., Specchia, S. and Cipiti, F., "Methane oxy-steam reforming reaction: Performances of Ru/γ-Al$_2$O$_3$ catalysts

loaded on structured cordierite monoliths", *Int. J. Hydrogen Energy*, **39**, 18592 (2014).

[13] Mondal, T., Pant, K. and Dalai, A., "Catalytic oxidative steam reforming of bio-ethanol for hydrogen production over Rh promoted Ni/CeO$_2$- ZrO$_2$ catalyst", *Int. J. Hydrogen Energy*, **40**, 2529 (2015).

[14] Abdollahifar, M., Haghighi, M. and Alizadeh, R., "Thermodynamic modeling Tri-reforming of metane", *Iranian Journal of Chemical Engineering*, **9** (60), 20 (2012).

[15] Boukha, Z., Jimenez Gonzalez, C., de Rivas, B. and Lopez-Fonseca, R., "Synthesis, characterization and performance evaluation of spinel-derived Ni/Al$_2$O$_3$ catalysts for various methane reforming reactions", *Appl. Catal. B: Environmental*, **159**, 190 (2014).

[16] Morales-Cano, F., Lundegaard, L. F., Tiruvalam, R., Falsig, H. and Skjoth-Rasmussen, M., "Improving the sintering resistance of Ni/Al$_2$O$_3$ steam reforming catalysts by promotion with noble metals", *Appl. Catal. A: General*, **498**, 117 (2015).

[17] Moradi, P. and Parvini, M., "Preparation of Lanthanum-Nickel-Aluminium Perovskite Systems*and*their Application in Methane Reforming Reactions", *Iranian Journal of Chemical Engineering*, **3** (3), 29 (2006).

[18] Li, B., Li, H., Weng, W. Z., Zhang, Q., Huang, C. J. and Wan, H. L.,"Synthesis gas production from partial oxidation of methane over highly dispersed Pd/SiO$_2$ catalyst", *Fuel*, **103**, 1032 (2013).

[19] Li, C., Ying, W., Cao, F., Zhang, H. and Fang, D., "Effects of impregnation solvents on catalytic performance of Co-

Ru-ZrO$_2$/γ-Al$_2$O$_3$ catalyst for Fischer-Tropsch synthesis", *Petrol. Sci. Tech.*, **26**, 704 (2008).

[20] Negrier, F., Marceau, E., Che, M. and de Caro, D., "Role of ethylenediamine in the preparation of alumina-supported Ni catalysts from [Ni (en) $_2$(H$_2$O) $_2$] (NO$_3$)$_2$: from solution properties to nickel particles", *C. R. Chimi.*, **6**, 231 (2003).

[21] Bentaleb, F., Che, M., Dubreuil, A. C., Thomazeau, C. and Marceau, E., "Influence of organic additives on the properties of impregnation solutions and on nickel oxide particle size for Ni/Al$_2$O$_3$ catalysts", *Catal. Today*, **235**, 250 (2014).

[22] Bang, Y., Park, S., Han, S. J., Yoo, J., Song, J. H., Choi, J. H. and Song, I. K., "Hydrogen production by steam reforming of liquefied natural gas (LNG) over mesoporous Ni/Al$_2$O$_3$ catalyst prepared by an EDTA-assisted impregnation method", *Appl. Catal. B: Environmental*, **180**, 179 (2016).

[23] Gerbec, J. A., Magana, D., Washington, A. and Strouse, G. F., "Microwave-enhanced reaction rates for nanoparticle synthesis", *J. Am. Chem. Soc.*, **127**, 15791 (2005).

[24] Horikoshi, S. and Serpone, N., Microwaves in nanoparticle synthesis: Fundamentals and applications, Wiley-VCH, Berlin, (2013).

[25] Glaspell, G., Fuoco, L. and El-Shall, M. S., "Microwave synthesis of supported Au and Pd nanoparticle catalysts for CO oxidation", *J. Phys. Chem. B.*, **109**, 17350 (2005).

[26] Liu, X., Khinast, J. G. and Glasser, B. J., "Drying of supported catalysts for low melting point precursors: Impact of metal loading and drying methods on the metal

distribution", *Chem. Eng. Sci.*, **79**, 187 (2012).

[27] Guodong, W., Yunpeng, X., Zhusheng, X. and Zhijian, T., "Characterization and catalytic properties of the Ni/Al$_2$O$_3$ catalysts for aqueous-phase reforming of glucose", *Catal. Letts.*, **129**, 250 (2009).

[28] Tsyganok, A. I., Tsunoda, T., Hamakawa, S., Suzuki, K., Takehira, K. and Hayakawa, T., "Dry reforming of methane over catalysts derived from nickel-containing Mg-Al layered double hydroxides", *J. Catal.*, **213**, 191 (2003).

[29] Souza, A. E. A. M., Maciel, L. J. L., Cavalcanti, V. O., Filho, N. M. L. and Abreu, C. A. M., "Kinetic-operational mechanism to autothermal reforming of methane, *Ind. Eng. Chem. Res.,* **50**, 2585 (2011).

[30] Ho, S. C. and Chou, T. C., "The Role of anion in the preparation of nickel catalyst detected by TPR and FTIR spectra", *Ind. Eng. Chem. Res.,* **34**, 2279 (1996).

[31] Karim, M. R., Rahman, M. A., Miah, M. A. J., Ahmad, H., Yanagisawa, M. and Ito, M., "Synthesis of γ-Alumina particles and surface characterization", *The Open Colloid Sci. J.,* **4**, 32 (2011).

[32] Stoyanova, M., Konova, P., Nikolov, P., Naydenov, A., Christoskova, St. and Mehandjiev, D., "Alumina-supported nickel oxide for ozone decomposition and catalytic ozonation of CO and VOCs", *Che. Eng. J.,* **122**, 41 (2006).

[33] Mette, K., Kühl, S., Tarasov, A., Düdder, H., Kähler, K., Muhler, M., Schlögl, R. and Behrens, M., "Redox dynamics of Ni catalysts in CO$_2$ reforming of methane", *Catal. Today*, **242**, 101 (2015).

[34] Zhou, L., Li, L., Wei, N., Li, J. and Basset, J. M., "Effect of NiAl$_2$O$_4$ formation on Ni/Al$_2$O$_3$ stability during

dry reforming of methane", *Chem. Cat. Chem*., **7**, 2508 (2015).

[35] Kirjin, P. D., Synthesis of solid catalyst, Wiley-VCH, Weinheim (2009).

[36] Che, M., "From unit operations to elementary processes: A molecular and multidisciplinary approach to catalyst preparation", *Stud. Surf. Sci. Catal*., **130**, 115 (2000).